# Single-Molecule Kinetic Analysis of Oxygenation of Co(II) Porphyrin at Solution/Solid Interface

*Kristen N. Johnson, Ursula Mazur, and K. W. Hipps* *

Department of Chemistry and Materials Science and Engineering Program. Washington State University, Pullman, WA, 99163-6430, USA

*Email: hipps@wsu.edu

ABSTRACT

Kinetic analysis of surface reactions at the single molecule level is important for understanding the influence of the substrate and solvent on reaction dynamics and mechanisms, but it is difficult with current methods. Here we present a stochastic kinetic analysis of the oxygenation of cobalt octaethylporphyrin (CoOEP) at the solution/solid interface by monitoring fluctuations from equilibrium using scanning tunneling microscopy (STM) imaging. Image movies were used to monitor the oxygenated and deoxygenated state dwell times. The rate constants for CoOEP oxygenation are $k_a$ = 4.9×10$^{-6}$ s$^{-1}$·torr$^{-1}$ and $k_d$ = 0.018 s$^{-1}$. This is the first use of stochastic dwell time analysis with STM to study a chemical reaction and the results suggest that it has great potential for application to a wide range of surface reactions. Expanding these stochastic studies

to further systems is key to unlocking kinetic information for surface confined reactions at the molecular level -- especially at the solution/solid interface.

TOC GRAPHIC

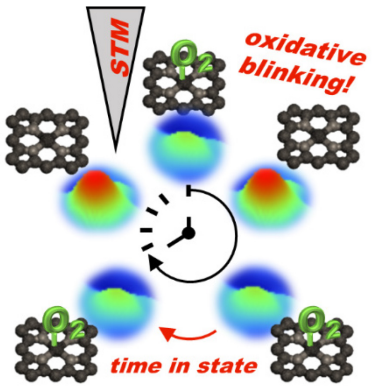


**KEYWORDS** single molecule kinetics, porphyrins, porphyrin oxygenation, scanning tunneling microscopy, surface chemical reactions, solution-solid interface.

Single molecule kinetic research is a unique field, special because of the ability to reveal the true, random nature of molecular scale processes. Additionally, single molecule techniques may resolve rare events that can expose insights into chemical mechanisms, and subpopulations in a system.[1] The literature concerning single molecule kinetics is well established for biochemical systems where one finds a fluorescent or binding moiety attached to a much larger biomolecule of interest in such a way as to not interfere with the biomolecule's function.[2-8] This approach is not possible with small molecules such as catalysts and tectons for self-assembly because the addition of a 'marker' group would certainly affect the chemical or physical process. Consequently, little is known about the reaction kinetics of smaller molecules at the molecular scale.

Herein, we show a detailed picture of the lifetime of oxygen complexed cobalt porphyrins using scanning tunneling microscopy at the solution/solid interface under ambient conditions. Under

these conditions, the porphyrin oxygenation state can be monitored in situ and in real time. Stochastic dwell time analysis of the oxygenated and deoxygenated state of cobalt(II)octaethylporphyrin (CoOEP) adsorbed on highly ordered pyrolytic graphite (HOPG) provides insight into the kinetics of complexation reactions on surfaces. This system was chosen because cobalt porphyrins, in addition to their use as mimics for the active iron porphyrin sites inside proteins and enzymes like hemoglobin,[9,10] have also been shown to be active for electrocatalytic reduction of oxygen when adsorbed on HOPG.[11-13] Metalated porphyrin and phthalocyanine systems have also been reported to act as gas sensors and as catalysts.[14,15] These important applications have made understanding porphyrin coordination chemistry a focus of the scientific community.

Applying the methods of analysis of fluorescence blinking to blinking observed in STM images opens a new paradigm for the field of single molecule kinetics. This approach is transformative for the field of STM based single molecule studies because it has been assumed that few chemical reactions can be studied kinetically at room temperature by STM. Temporal resolution of STM is relatively slow (of the order of seconds per image), but we show that the surface reaction kinetics can be extracted from STM images for reactions of practical interest. Further, the application of this method for deriving kinetic data from STM images of systems at equilibrium can provide new insight into the kinetics of surface reactions in the presence of solvents at ambient conditions.

Previously, the oxygenation of CoOEP at the phenyloctane/HOPG interface was observed to be a reversible process that obeys the Langmuir adsorption isotherm.[16] The reaction occurs when the CoOEP molecule is adsorbed on the HOPG surface but not in solution phase. Computational studies have shown that this is because the HOPG surface acts as an electron donating ligand that stabilizes the ligated product.[17] Surface adsorption-desorption reactions have been studied using

the Langmuir adsorption framework extensively and are described by the chemical reaction equation

$$L + S \underset{k_d}{\overset{k_a}{\rightleftarrows}} LS$$

where *L* is the adsorbate or in this case ligand in solution, *S* is an unoccupied surface site and *LS* is an occupied surface site.[18] An important assumption in this model is that all unoccupied sites are equivalent. In this system, *S* is an unreacted CoOEP and *LS* is an oxygenated CoOEP. The forward reaction rate constant $k_a$ depends both on the concentration of ligands in solution and the number of unfilled surface sites. The reverse reaction rate constant $k_d$ depends only on the number of reacted porphyrin molecules. The corresponding kinetic equation is

$$\frac{dN_{LS}}{dt} = k_a P_{O2} N_S - k_d N_{LS}$$

Dividing by the area of the surface and setting $k_a' = k_a P_{O_2}$

$$\frac{d\theta}{dt} = k_a'(1-\theta) - k_d\theta$$

where *N* denotes number and indices denote the species, $\theta$ is the fraction of reacted surface sites and $P_{O_2}$ is the partial pressure of oxygen. The concentration of $O_2$ in solution can be related to the partial pressure above the solution through Henry's law.

In a series of STM images, the reaction appears as CoOEP molecules cycling between a dark, oxygenated state and a bright, deoxygenated state. This is due to oxygen attenuation of the tunneling current signal, which occurs through the half-filled $d_z^2$ orbital on the Co atom.[16] An example sequence of STM images is shown in **Fig. 1.** From a stochastic viewpoint, the oxygenation reaction can be viewed as a series of Bernoulli trials where the probability of a successful transition between the ligated and unligated states is related to the stochastic rate constants.[1]

If the system is Markovian, meaning the behavior of the system depends only on the current state and not on the state history, dwell times in each state are distributed according to an exponential distribution

$$P(t_i|k_i) = k_i e^{-k_i t_i}$$

Where $P(t_i|k_i)$ is the probability density function (PDF) of molecule in $i^{th}$ state for dwell time lasting time $t_i$ ,*a*nd $k_i$ is the stochastic rate constant.[5,19] The mean of the exponential distribution, or mean dwell time, is $1/k_i$ and therefore is used to determine the stochastic rate constants. It follows from the Onsager's Regression Hypothesis that as a system approached equilibrium,

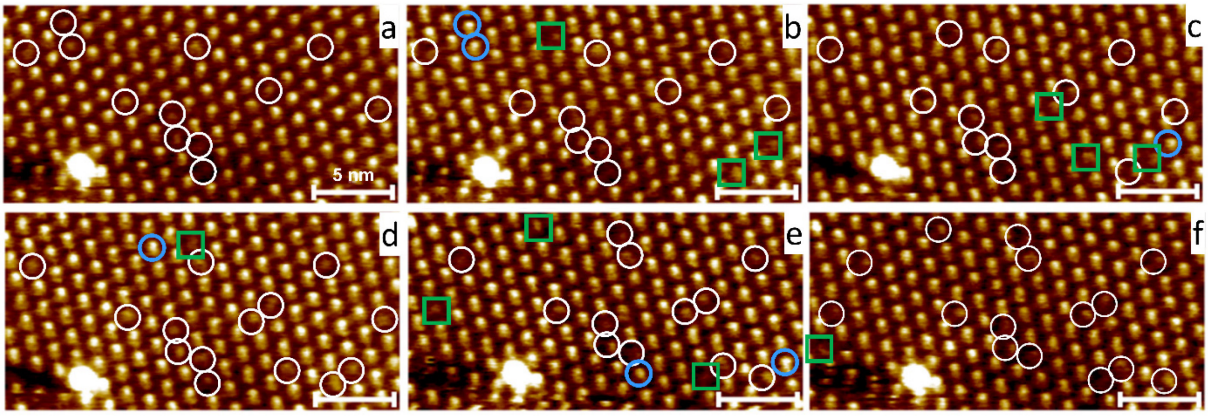


**Figure 1.** Example STM image sequence collected from a-f at a rate of 32 s/image showing transitions between ligation states between images. White circles denote CoOEP molecules in the bound state that stayed in the bound state, green squares denote the unbound to bound transition and blue circles denote the bound to unbound transition. Tunneling conditions $V_{bias}$ = +0.5V, $I_{current}$ = 20 pA and scale bar is 5 nm. The large bright feature in the bottom left corner is a defect used for image registration.

fluctuations in the state of individual molecules behave in the same way as an ensemble system does.[20] Moreover, from the ergodic hypothesis, a single molecule dwell time distribution is equivalent to the aggregate of many identical molecules dwell times.[21] These concepts form the basis of methods that have been used for studying cell membrane ion channel kinetics via current measurements[6], protein folding kinetics via force clamp spectroscopy[4], and redox reaction kinetics via fluorescence spectroscopy[2], but have not been applied to chemical processes observed by STM.

In order to apply these ideas to the $O_2$-CoOEP/HOPG system, the state dwell times for a total of 618 molecules observed for between 15 and 70 minutes were determined experimentally from sequences of STM images, collected at a rate of 32s per image. First, the image sequence was registered so that a marker point, present in all images, was aligned in space and then the image was fit to a unit cell grid with one CoOEP per grid cell. This grid was used to keep track of each molecule throughout the image sequence and the average height value within a grid cell was used to determine a cutoff threshold to identify the dark, ligated CoOEP molecules. The state sequences (many sequences like the one shown in **Fig. 2**) were inspected in order to obtain dwell times for both the bound and unbound states. Dwell time histograms shown in **Fig. 3** were fit with the exponential PDF where the mean of the fitted distribution is the mean dwell time. We found that the mean dwell time for the ligated state is much shorter than the dwell time in the unligated state, 66 s and 474 s respectively. Since the mean of the exponential distribution is

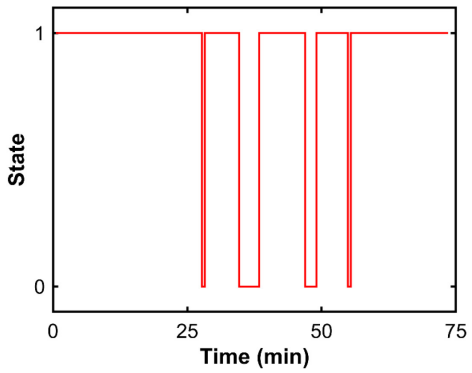


**Figure 2**. Representative idealized state sequence of one CoOEP molecule tracked for 138 images. Dwell time histograms are built up by examining many state traces. State 1 = deoxygenated and state 0 = oxygenated.

$1/k_i$ this gives stochastic rate constants of 0.002 $s^{-1}$ for the forward reaction and 0.017 $s^{-1}$ for the reverse reaction.

STM is an excellent tool for achieving sub-molecular resolution and the ability to resolve the ligation state of many molecules simultaneously, however, the time resolution is on the order of 10s of seconds per scan. The time resolution may be increased,[22,23] but usually with fewer molecules in each image and greater difficulty in long time tracking. Missed dwells arise from sampling time limitations and cause the reported rate constants to appear smaller than reality. For example, take a reversible two state system with states *A* and *B*. A missed dwell in state *A* causes a missed transition out of state *B* and can lead to erroneously long dwells in state *B*. A rule of thumb is that in order for results to be relatively free of the effects of missed dwells the rate constant multiplied by the image collection time should be less than 0.1.[19] For the data reported here, the smallest $k\tau = 0.002\ s^{-1} \times 32\ s = 0.07$ uncomfortably close to 0.1. Fortunately, the missed dwell issue has been addressed previously and can be accounted for by creating an augmented network where missed dwells are considered with virtual states.[19,24,25] Since the dwell times are distributed according to the exponential PDF, the fraction of dwell times

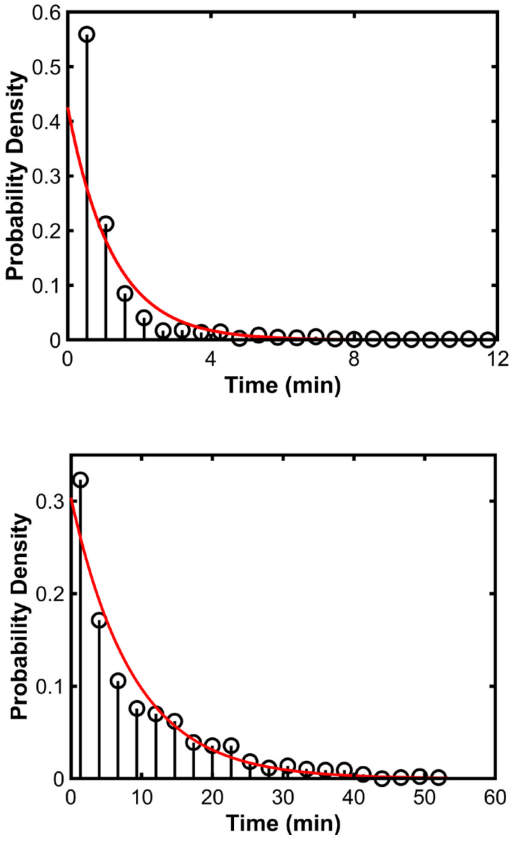


**Figure 3.** Dwell time distributions for the time spent in oxygenated state (upper) and deoxygenated state (lower). Distributions have been fit with exponential probability distributions with mean dwell times of 60 s and 470 s, respectively. Circles denote histogram bin centers.

that are missed $f_{\text{missed}}$ in state *A* is the fraction of dwell times too short to capture in state *B*. That fraction is found by considering the area of the distribution less than the scan time which is[24]

$$f_{missed,A} = \int_{t=0}^{\tau_c} k_{B\to A} e^{-k_{B\to A}t}\,\mathrm{dt} = 1 - e^{-k_{B\to A}\tau_c}$$

where $k_{B\to A}$ is the rate constant for the transition from state *B* to state *A* and $\tau_c$ is the cutoff time which is the shortest dwell time that can be captured by the employed method. Here we take $\tau_c$ to be one half the image collection time. The corrected rate constant $k_{\text{corrected}}$ can be determined by assuming that the corrected rate constant for the *A* to *B* transition can be partitioned using a virtual state to account for $k_{\text{missed}}$ by the following[19,24]

$$k_{\text{corrected}} = k_{\text{missed}} + k_{\text{observed}}$$

$$k_{\text{corrected},,A\to B} = f_{\text{missed},\,B} \times k_{\text{corrected},\,B\to A} + k_{\text{observed},\,A\to B}$$

This results in a set of coupled equations, one equation for each state that can be solved numerically through a least squares method in order to correct the rate constants from the effects of missed dwells. With correction, rate constants are improved to ~90% accuracy even when rate

**Table 1.** Results of dwell time analysis

| | **CoOEP** | **$O_2$-CoOEP** |
|---|---|---|
| $N_{\text{total instances}}$ | 14329 | 1882 |
| $N_{\text{transitions out}}$ | 870 | 1012 |
| mean dwell time (s) | 470±5 | 60±5 |
| observed rate constant ($s^{-1}$) | $k_a$' = 0.002± 0.001 | $k_d$ =0.017± 0.001 |
| corrected rate constant ($s^{-1}$) | $k_a$' = 0.003± 0.001 | $k_d$ = 0.018± 0.001 |

constants are similar to the acquisition rate.[19] The corrected rate constants for CoOEP oxygenation are $k_a'$ = 0.003 $s^{-1}$ and $k_d$ = 0.018 $s^{-1}$. Note that the corrected rate constants fall within the error bars of the uncorrected version – even though $k\tau \sim 0.1$. The results of the dwell time analysis are collected in **Table** 1. These results demonstrate that single-molecule reactions of a reversible surface-confined system can be studied with STM despite the seemingly poor temporal resolution of the experiment.

In the image sequences, individual molecules transition between the ligated and unligated states, but the average number of total ligated CoOEP molecules remains constant in time at nearly 8% ligated CoOEP. The constant coverage with time indicates that the system is in dynamic equilibrium, as is required for this method of analysis. The equilibrium constant derived from the dwell time analysis is $K = k_a/k_d = 3\times10^{-4}$ $torr^{-1}$. Because it is common to do so in the solution-phase oxygen-binding literature, we used our data to determine the $P_{1/2}$(298 K), the $O_2$ partial pressure at which half the sites on the CoOEP/HOPG surface would be oxygenated. We found that $P_{1/2}$(298 K) = 3300 Torr. Comparing the present kinetic results with the results for the same system determined by Langmuir adsorption isotherm analysis, $P_{1/2}$ and $\Delta G$ values agree nicely, **Table 2**.[16] The standard state is the conventional choice for this type of process, 1 torr partial pressure of oxygen, and 0.5 $O_2$-CoOEP coverage.[10,26,33]

Although the CoOEP/HOPG system binds $O_2$ much more strongly than CoOEP in solution, it still does not compete with porphyrins specially designed for oxygen binding, the picket-fence porphyrins.[26,27] At room temperature a $P_{1/2}$ of 70 Torr was reported for Co(TpivPP)(A-MeIm) in toluene.[26] We note that rate constants for this porphyrin binding oxygen in solution determined by transient adsorption spectroscopy are orders of magnitude larger than what we report here.[27] . Clearly, the influence of the substrate is enough to allow oxygen binding at room temperature but

does not do as well at stabilizing the oxygenated species as the binding pocket mimicking picket-fence porphyrin. The combination of enhanced binding with slowed kinetics illustrates the intriguing nature of reaction dynamics for species absorbed on HOPG and warrants further study.

**Table 2.** Comparison of Thermodynamic Properties for Oxygenation of Various Porphyrins at 298 K

| | **CoOEP (this work)** | **CoOEP (at PO/HOPG)[a]** | **Co "Picket-fence" porphyrin (in toluene)[b]** |
|---|---|---|---|
| $P_{1/2}$ (torr) | 3300 | 3200 | 140 |
| $\Delta G$ (KJ/mol)[c] | 20 ± 0.5 | 21 ± 0.5 | 12.8 ± 0.5 |

a) From Reference 16; b) From Reference 26; c) Standard State 1 torr $O_2$ and 0.5 $O_2$-CoOEP coverage

It is useful to consider the collision frequency between the oxygen molecules in solution and the CoOEP monolayer. Campbell et al has described a method for calculating the collision frequency between a solute and a surface from solution.[28] Using Campbell's method the flux of oxygen molecules to the surface was calculated to be $2.0\times10^{22}$ collision/cm$^2$s at ~5 mM concentration of oxygen molecules in solution, calculated by Henry's Law for $P_{O_2}$= 608 torr. The Henry's Law constant values are not available for phenyloctane, but are available for two related solvents, octane and toluene.[29,30] Since the cross-sectional area of the cobalt atom (0.072 nm$^2$)[31] accounts for 4.2% of the area per CoOEP molecule on HOPG (1.72 nm$^2$) the collision rate between dioxygen molecules and cobalt metal centers is $1.4\times10^8$ collision/s. If every collision of oxygen with a cobalt atom resulted in the formation of a complex the adsorption reaction rate would be expected to be on the order of $10^8$ s$^{-1}$; however, this is not the case. Based on the observed rate of adsorption,

0.003 $s^{-1}$ at present $O_2$ pressure, only 1 in $10^{11}$ collisions results in the formation of an oxygenated porphyrin complex. This is a markedly different result than that observed by transient adsorption spectroscopy with the picket-fence porphyrin. This may be indicative of the importance of the protein-binding pocket mimicking pivalamidophenyl groups, ("pickets") utilized in the molecule. Most cobalt porphyrins (other than myoglobin[10] and picket fence style porphyrins[26,32]) do not form oxygen complexes in solution at room temperature.[33] This is also true for the cobalt octaethylporphyin where the electron donation from the substrate is essential for stabilizing the complex.[16] Substrate stabilization has also been observed by those studying gas sensors[34] and selective gas membranes[35].

Tip influences on rates were considered and ruled out by testing the scan speed dependence of the average number of $O_2$-CoOEP molecules within a single frame. We tested image collection time between 30 and 240 seconds and did not see any change in the mean number of $O_2$-CoOEP in each frame. As the scan speed decreases the amount of time the STM tip spends interacting with each individual molecule increases. If the tip electric field or a tip induced inelastic excitation was inducing deoxygenation of the CoOEP molecules, then we would expect to observe fewer $O_2$-CoOEP molecules as the image collection time increases. Since this is not observed we have ruled out a significant influence of tip induced desorption on the observed rates.

Conceptually there is no difference between monitoring a single molecule for a long time or the dynamics of many molecules for a shorter amount of time. In theory either approach is valid and feasible. The influence of thermal drift at the liquid-solid interface is an issue for both methods but especially so when monitoring a single molecule for an extended time because there is no guarantee that the molecule being observed is the same molecule across the entire observation time. This is why we have opted to monitor multiple molecules at a time because it allows us to include a tracer in all the images which removes the influence of thermal drift and ensures that the molecules are the same throughout the image sequence. The

advantage to immobilizing the STM-tip on top of a single molecule is that the time resolution can be improved greatly up to the response time of the STM pre-amp. Another issue, perhaps even more critical, with using a fixed tip position to monitor chemical processes (as opposed to physical changes) is that the tip body will physically limit the diffusion of $O_2$ (or other reagent) to the apex position of the tip. Thus, the local concentration will likely change with time and deviate from the solution concentration. Also, any field induced effects on the adsorbate-surface complex will be amplified by the constant presence of the tip.

Although the stochastic method is well established in the biophysical field where the molecules are large enough to attach fluorescent tags without compromising the chemistry of the parent molecule, it has rarely been applied to single small molecule reactions. This study is the first example of using dwell time analysis to study chemical reaction kinetics with STM. We note that STM has been used in a similar manner, but to study the **physical kinetics** of rotation of acetylene and diffusion of hydrogen on Cu(001) in vacuum at low temperature.[36,37] It has long been assumed that STM cannot be used to study chemical kinetics at ambient conditions in this way because of constraints on image collection time. However, we have shown: 1) Surface reactions can proceed orders of magnitude slower than expected based on solution phase kinetic measurement, and 2) it is possible to correct rate constants for the effects of missed dwells due to low temporal resolution thereby extending the range of rates that can be measured. Lest one assume that the $O_2$-CoOEP/HOPG system is unique, we have tracked adsorption and desorption events in time for several systems including 1-phenylimidazole-CoOEP/HOPG,[38] 4-methoxypyridine-CoOEP/HOPG,[39] and imidazole-NiOEP/HOPG.[17] Thus, these systems are excellent candidates for stochastic analysis and that work is underway. This study shows that STM can be used for dwell time analysis and will expand the types of reactions that can be kinetically studied at the single molecule level. Further studies of this type on other surface reactions will clarify the role of the

surface in chemical reactions and its influence on reaction rates as well as allow for new mechanistic studies to be undertaken.

**Experimental Details**:

In all STM experiments a freshly cleaved HOPG surface (1 $cm^2$, ZYA grade from Tips Nano) was exposed to a 10 μL volume of 10 μM solution of CoOEP in phenyloctane solvent. 2,3,7,8,12,13,17,18-Octaethyl-21H,23H-porphine cobalt(II) was acquired from Aldrich. Phenyloctane (99%) from TCI Organics. The entire STM experiment was housed in an environmental chamber and all experiments were performed under 80% oxygen 20% argon atmosphere, giving and oxygen partial pressure of 608 torr, after 2 hour equilibration time. STM tips were made by mechanically cutting $Pt_{0.8}Ir_{0.2}$ wire (California Fine Wire Company Grover Beach, Ca.).

AUTHOR INFORMATION

The authors declare no competing financial interests.

Authors

**Kristen N. Johnson** − Department of Chemistry and Materials Science and Engineering Program, Washington State University, Pullman, Washington 99163-4630, United States; orcid.org/0000-0003-3622-9686.

**Ursula Mazur** − Department of Chemistry and Materials Science and Engineering Program, Washington State University, Pullman, Washington 99163-4630, United States; orcid.org/0000-0002-3471-4883

**K. W. Hipps** − *Department of Chemistry and Materials Science and Engineering Program, Washington State University, Pullman, Washington 99163-4630, United States;* orcid.org/0000-0002-5944-5114.

ACKNOWLEDGMENT

This works is supported by the US National Science Foundation in the form of grant CHE1807225. Thank you to Kirill Gurdumov for helpful discussions and to Jake Bailey for assistance with data analysis.

REFERENCES

(1) Resnick, S. I. *Adventures in Stochastic Processes*, 2nd ed.; Birkhäuser, 2002; pp 1- 626.

(2) Kawai, K.; Fujitsuka, M.; Maruyama, A. Single-Molecule Study of Redox Reaction Kinetics by Observing Fluorescence Blinking. *Acc. Chem. Res.* **2021**, *54* (4), 1001–1010. https://doi.org/10.1021/ACS.ACCOUNTS.0C00754.

(3) Elf, J.; Barkefors, I. Single-Molecule Kinetics in Living Cells. *Annu. Rev. Biochem.* **2019**, *88* (1), 635–659. https://doi.org/10.1146/annurev-biochem-013118-110801.

(4) Brujić, J.; Hermans, R. I. Z.; Garcia-Manyes, S.; Walther, K. A.; Fernandez, J. M. Dwell-Time Distribution Analysis of Polyprotein Unfolding Using Force-Clamp Spectroscopy. *Biophys. J.* **2007**, *92* (8), 2896–2903. https://doi.org/10.1529/biophysj.106.099481.

(5) Colquhoun, D.; Hawkes, A. G. The Principles of the Stochastic Interpretation of Ion-Channel Mechanisms. In *Single-Channel Recording*; Sakmann, B., Neher, E., Eds.; Springer, 1995; pp 397–482. https://doi.org/10.1007/978-1-4419-1229-9

(6) Ball, F. G.; Rice, J. A. Stochastic Models for Ion Channels: Introduction and Bibliography. *Math. Biosci.* **1992**, *112* (2), 189–206. https://doi.org/10.1016/0025-5564(92)90023-P.

(7) Lam, K. T.; Taylor, E. L.; Thompson, A. J.; Ruepp, M. D.; Lochner, M.; Martinez, M. J.; Brozik, J. A. Direct Measurement of Single-Molecule Ligand-Receptor Interactions. *J. Phys. Chem. B* **2020**, *124* (36), 7791–7802. https://doi.org/10.1021/ACS.JPCB.0C05474.

(8) Wu, S.; Zhang, W.; Li, W.; Huang, W.; Kong, Q.; Chen, Z.; Wei, W.; Yan, S. Dissecting the Protein Dynamics Coupled Ligand Binding with Kinetic Models and Single-Molecule FRET. *Biochemistry* **2022**, *61* (6), 433–445. https://doi.org/10.1021/ACS.BIOCHEM.1C00771.

(9) Alberti, M. N.; Polyhach, Y.; Tzirakis, M. D.; Tödtli, L.; Jeschke, G.; Diederich, F. Exploring the Strength of the H-Bond in Synthetic Models for Heme Proteins: The Importance of the N−H Acidity of the Distal Base. *Chem. - A Eur. J.* **2016**, *22* (29), 10194–10202. https://doi.org/10.1002/chem.201601505.

(10) Collman, J. P.; Fu, L. Synthetic Models for Hemoglobin and Myoglobin. *Acc. Chem. Res.* **1999**, *32* (6), 455–463. https://doi.org/10.1021/ar9603064.

(11) Ye, L.; Fang, Y.; Ou, Z.; Xue, S.; Kadish, K. M. Cobalt Tetrabutano- and Tetrabenzotetraarylporphyrin Complexes: Effect of Substituents on the Electrochemical Properties and Catalytic Activity of Oxygen Reduction Reactions. *Inorg. Chem.* **2017**, *56* (21), 13613–13626. https://doi.org/10.1021/acs.inorgchem.7b02405.

(12) Yamazaki, S. I.; Yamada, Y.; Ioroi, T.; Fujiwara, N.; Siroma, Z.; Yasuda, K.; Miyazaki, Y. Estimation of Specific Interaction between Several Co Porphyrins and Carbon Black: Its Influence

on the Electrocatalytic $O_2$ Reduction by the Porphyrins. *J. Electroanal. Chem.* **2005**, *576* (2), 253–259. https://doi.org/10.1016/j.jelechem.2004.10.022.

(13) Saran, N.; Thomas, T. L.; Bhavana, P. Dioxygen Reduction Using Electrochemically Reduced Graphene Oxide - Polymerized Cobalt-4-Pyridylporphyrin Composite. *Int. J. Hydrogen Energ.* **2022**, *47* (28), 13629-13640. https://doi.org/10.1016/j.ijhydene.2022.02.109.

(14) Zhang, W.; Lai, W.; Cao, R. Energy-Related Small Molecule Activation Reactions: Oxygen Reduction and Hydrogen and Oxygen Evolution Reactions Catalyzed by Porphyrin- and Corrole-Based Systems. *Chem. Rev.* **2017**, *117* (4), 3717–3797. https://doi.org/10.1021/acs.chemrev.6b00299.

(15) Paolesse, R.; Nardis, S.; Monti, D.; Stefanelli, M.; Di Natale, C. Porphyrinoids for Chemical Sensor Applications. *Chem. Rev.* **2017**, *117* (4), 2517–2583. https://doi.org/10.1021/acs.chemrev.6b00361.

(16) Friesen, B. A.; Bhattarai, A.; Mazur, U.; Hipps, K. W. Single Molecule Imaging of Oxygenation of Cobalt Octaethylporphyrin at the Solution/Solid Interface: Thermodynamics from Microscopy. *J. Am. Chem. Soc.* **2012**, *134* (36), 14897–14904. https://doi.org/10.1021/ja304431b.

(17) Nandi, G.; Chilukuri, B.; Hipps, K. W.; Mazur, U. Surface Directed Reversible Imidazole Ligation to Nickel(II) Octaethylporphyrin at the Solution/Solid Interface: A Single Molecule Level Study. *Phys. Chem. Chem. Phys.* **2016**, *18* (30), 20819–20829. https://doi.org/10.1039/C6CP04454A.

(18) Hsu, J. P.; Sun, S. S. A Probabilistic Analysis of the Adsorption of Particles on Solid Surfaces. *J. Colloid Interf. Sci.* **1988**, *122* (1), 73–77. https://doi.org/10.1016/0021-9797(88)90288-3.

(19) Kinz-Thompson, C. D.; Bailey, N. A.; Gonzalez, R. L. Precisely and Accurately Inferring Single-Molecule Rate Constants. *Methods Enzymol.* **2016**, *581*, 187–225. https://doi.org/10.1016/bs.mie.2016.08.021.

(20) Hernández, E. S. *Nonequilibrium Statistical Mechanics*; Oxford University Press, 1990; pp 1–203.

(21) Gillespie, D. T. Stochastic Simulation of Chemical Kinetics. *Annu. Rev. Phys. Chem.* **2007**, *58* (1), 35–55. https://doi.org/10.1146/annurev.physchem.58.032806.104637.

(22) Strohmaier, R.; Ludwig, C.; Petersen, J.; Gompf, B.; Eisenmenger, W.; Scanning Tunneling Microscope Investigations of Lead-phthalocyanine on $MoS_2$. *J. Vac. Sci. Technol. B*, **1996**, *14* 1079-1082.

(23) Rost, M. J. High-Speed Electrochemical STM. In *Encyclopedia of Interfacial Chemistry: Surface Science and Electrochemistry*; Wandelt, K., Ed.; Elsevier, **2018**; pp 180-198.

(24) Crouzy, S. C.; Sigworth, F. J. Yet Another Approach to the Dwell-Time Omission Problem of Single-Channel Analysis. *Biophys. J.* **1990**, *58* (3), 731–743. https://doi.org/10.1016/S0006-3495(90)82416-4.

(25) Stigler, J.; Rief, M. Hidden Markov Analysis of Trajectories in Single-Molecule Experiments and the Effects of Missed Events. *ChemPhysChem.* **2012**, *13* (4), 1079–1086. https://doi.org/10.1002/CPHC.201100814.

(26) Collman, J. P.; Brauman, J. I.; Doxsee, K. M.; Halbert, T. R.; Hayes, S. E.; Suslick, K. S. Oxygen Binding to Cobalt Porphyrins. *J. Am. Chem. Soc.* **1978**, *100* (9), 2761–2766. https://doi.org/10.1021/ja00477a031.

(27) Zou, S.; Baskin, J. S.; Zewail, A. H. Molecular Recognition of Oxygen by Protein Mimics: Dynamics on the Femtosecond to Microsecond Time Scale. *P. Natl. Acad. Sci. USA* **2002**, *99* (15), 9625–9630. https://doi.org/10.1073/pnas.152333399.

(28) Jung, L. S.; Campbell, C. T. Sticking Probabilities in Adsorption of Alkanethiols from Liquid Ethanol Solution onto Gold. *J. Phys. Chem. B* **2000**, *104* (47), 11168–11178. https://doi.org/10.1021/jp001649t.

(29) Li, A.; Tang, S.; Tan, P.; Liu, C.; Liang, B. Measurement and Prediction of Oxygen Solubility in Toluene at Temperatures from 298.45 K to 393.15 K and Pressures up to 1.0 MPa. *J. Chem. Eng. Data* **2007**, 52, 2339−2344. https://doi:10.1021/je700330c

(30) Battino, R.; Rettich, T. R.; Tominaga, T. The Solubility of Oxygen and Ozone in Liquids. *J. Phys. Chem*. *Ref. Data* **1983**, 12, 163−178. https://doi:10.1063/1.555680

(31) Clementi; E.; Raimondi, D. L.; Reinhardt, W. P. Atomic Screening Constants from SCF Functions. II. Atoms with 37 to 86 Electrons. *J. Chem. Phys.,* **1967** 47 (4): 1300–1307. https:\\doi:10.1063/1.1712084.

(32) Collman, J. P.; Brauman, J. I.; Iverson, B. L.; Sessler, J. L.; Morris, R. M.; Gibson, Q. H. $O_2$ and CO Binding to Iron(II) Porphyrins: A Comparison of the “Picket Fence” and “Pocket” Porphyrins. *J. Am. Chem. Soc.* **1983**. https://doi.org/10.1021/ja00348a019.

(33) Walker, F. ESR Studies of Co(II) Tetraphenylporphyrins and Their Oxygen Adducts: Complex Formation with Aromatic Molecules and Sterically Hindered Lewis Bases. *J. Magn. Reson.* **1974**, *15* (2), 201–218. https://doi.org/10.1016/0022-2364(74)90072-9.

(34) Hyakutake, T.; Okura, I.; Asai, K.; Nishide, H. Dual-Mode Oxygen-Sensing Based on Oxygen-Adduct Formation at Cobaltporphyrin–Polymer and Luminescence Quenching of Pyrene: An Optical Oxygen Sensor for a Practical Atmospheric Pressure. *J. Mater. Chem.* **2008**, *18* (8), 917. https://doi.org/10.1039/b716073a.

(35) Suzuki, Y.; Nishide, H.; Tsuchida, E. Membranes of the Picket Fence Cobalt Porphyrin Complexed with Poly(Vinylimidazole and -Pyridine)s: Selective Optical Response to Oxygen. *Macromolecules* **2000**, *33* (7), 2530–2534. https://doi.org/10.1021/ma9917949.

(36) Lauhon, L. J.; Ho, W. Single Molecule Thermal Rotation and Diffusion: Acetylene on Cu(001). *J. Chem. Phys.*, **1999**, *111*, 5633. https://doi.org/10.1063/1.479863.

(37) Lauhon, L. J.; Ho, W. Direct Observation of the Quantum Tunneling of Single Hydrogen Atoms with a Scanning Tunneling Microscope. *Phys. Rev. Lett.,* **2000**, 85, 4566. https://doi.org/10.1103/PhysRevLett.85.4566.

(38) Korpany, K. V.; Chilukuri, B.; Hipps, K. W.; Mazur, U. Cooperative Binding of 1-Phenylimidazole to Cobalt(II) Octaethylporphyrin on Graphite: A Quantitative Imaging and Computational Study at Molecular Resolution. *J. Phys. Chem. C* **2020**, *124* (34), 18639–18649. https://doi.org/10.1021/acs.jpcc.0c05516.

(39) Johnson, K. N.; Hipps, K. W.; Mazur, U. Quantifying Reversible Nitrogenous Ligand Binding to Co(II) Porphyrin Receptors at the Solution/Solid Interface and in Solution. *Phys. Chem. Chem. Phys.* **2020**, *22* (42), 24226–24235. https://doi.org/10.1039/d0cp04109b.